Chalcogenide Letters Vol. 7, No. 6, June 2010, p. 431-438

EFFECT OF THICKNESS ON STRUCTURAL AND OPTICAL PROPERTIES OF THERMALLY EVAPORATED CADMIUM SULFIDE POLYCRYSTALLINE THIN FILMS

ZIAUL RAZA KHAN, M. ZULFEQUAR, MOHD. SHAHID KHAN*
Department of Physics, Jamia Millia Islamia (Central University), New Delhi-110025, India

Cadmium sulfide polycrystalline thin films of different thickness were deposited on ultrasonically cleaned glass substrates by thermal evaporation technique in a vacuum of about $2x10^{-5}$ torr. X-ray diffraction and SEM (scanning electron microscope) were used to characterize the thin films. X-ray diffraction study showed that, all the films have the hexagonal wurtzite structure, with lattice constants a=b=4.142, c=6.724A°. Crystallite sizes calculated from Scherrer relation are in the range of 49-68 nm and the grain size of the thin films are observed to increase with the increase in the thickness of the sample. The optical properties of the polycrystalline thin films were investigated by the UV-VIS-NIR spectroscopy. The band gap of the thin films is found to be direct allowed transition and increases with the increase of thickness of films in the range of 2.35- 2.46 eV. Extinction coefficient k showed oscillatory behavior in lower band edge region. The CdS polycrystalline thin films are suitable for solar cell application.

(Received June 1, 2010; accepted June 26, 2010)

Keywords: CdS, polycrystalline, SEM, grain size, thin films

1. Introduction

The synthesis and characterization of polycrystalline materials have attracted much attention not only because of their exceptional properties [1, 2], but also due to their structure and temperature dependent properties and great potential for many technological applications [3, 4]. Recently, there has been an increase in research and development of II-VI materials which are widely used in devices such as interference filters, optical fibers, optical instruments, coated glazing for windows, solar energy collectors and low coast flat panel solar cells. Optical constant as input data in design process of the thin film devices gives the designer an additional tool for optimization of the product design, and thus an accurate knowledge of optical constant over wide range of wavelength is essentially important [5, 6].

These films offer a larger number of applications in solid-state device technologies such as the target material of television cameras, microwave devices, switching devices, infrared detectors, diodes and Hall effect devices.

Many techniques have been reported for the deposition of CdS thin films. These include thermal evaporation [7], sputtering [8], chemical bath deposition [9], spray pyrolysis [10], metal organic chemical vapour deposition (MOCVD) [11], molecular beam epitaxial technique [12], electro deposition [13], photochemical deposition [14] etc. The structural and physical properties of CdS thin films prepared by thermal evaporation technique at different deposition conditions have been reported in literature [15-18]. In this work, thermal evaporation technique has been chosen for deposition of CdS thin films because it is a trouble-free and controllable technique. The present study is centred over the effect of thickness on the structural and optical properties of thermally evaporated CdS polycrystalline thin films. X-Ray diffraction (XRD), Ultraviolet-visible

*Corresponding author: mskhan@jmi.ac.in; shahidkhan_m@yahoo.com

(UV–VIS-NIR) and Scanning Electron Microscope (SEM) are used to characterize the samples. Optical constants, such as optical band gap, absorption coefficient, extinction coefficient, Urbach's energy and grain size are evaluated from the optical spectra.

2. Experimental

Analytical grade CdS (99.99% purity) was purchased from Alfa Aesar Company (UK). CdS thin films were prepared by thermal evaporation technique using vacuum coating unit in a vacuum about 2×10^{-5} Torr. CdS was put in a Molybdenum boat and the substrate glass was placed directly above the source at a distance of nearly 18 cm. The glass substrates were cleaned with freshly prepared acetone, detergent solution and distilled water. Further, the substrates were subjected to ultrasonically cleaning prior to the evaporation of CdS. Thickness of the thin films were measured with a Gaertner Scientific Corporation Chicago-L117 Spectroscopic Ellipsometer (SE). The optical absorbance and transmission spectra for as-deposited CdS thin films of different thickness were obtained in the ultraviolet/ infrared region up to 900 nm using JASCO UV-VIS-NIR spectrometers (V-570). The optical measurements were made at room temperature with uncoated glass slide as reference. The structure of the films was studied by the using Philips analytical diffractometer (Model- PW3710). Surface morphology of the films was characterized by scanning electron microscopy (Jeol Scanning Microscope-6380).

3. Results and discussion

The thickness of the four CdS thin films deposited on glass substrate as measured using SE was found to be 200 nm, 245 nm, 400 nm and 500 nm. Effect of the change in thickness of the film on the structural and optical properties using the XRD and UV-VIS absorption spectroscopy are presented in the following sections.

3.1 X-ray diffraction analysis

Fig. 1 shows the X-ray diffraction patterns of the four CdS thin films deposited on glass substrate. Deposited films were uniform, reflective, adherent and orange in colour. A strong peak with 2θ value about 26.4˚ corresponds to the (002) crystalline plane of CdS is present in all the four XRD patterns. This peak in these XRD could be indexed to hexagonal structure of CdS and the 2θ value is consistent with the value in standard card (JCPDS file no. 41-1049).
The crystallites size of the grains in the films is estimated using the Sherer formula [10] :

$$D = \frac{K\lambda}{\beta_{2\theta} \cos\theta} \tag{1}$$

where K is a constant taken to be 0.94, λ the wavelength of X-Ray used (λ=1.54 Å), $\beta_{2\theta}$ the full width at half maximum of (002) peak of X-RD pattern, and 2θ is the Bragg angle. . The values of crystallites sizes are found to be in the range 49-68 nm. A weak peak at θ=47˚ corresponding to (110) plane is also observed in the XRD pattern. Using the Miller indices of these planes, the lattice parameters a=b and c of the unit cell are evaluated according to the relation:

$$\frac{1}{d^2} = \frac{4}{3}\frac{h^2 + hk + l^2}{a^2} + \frac{l^2}{c^2} \tag{2}$$

where d is the interplanar spacing, and (h,k,l) are the Miller indices.. The calculated value of the lattice parameter are a=b=4.142, and c=6.724A˚.
The strain (ε) of the films is determined with the use of the following formula:

$$\varepsilon = \frac{\beta \cos\theta}{4} \tag{3}$$

The values of 2θ, $\beta_{2\theta}$ the full width at half maximum, interplanar spacing d, grain size, strain and intensity of the XRD peak in the thin films of different thickness are given in table 1.

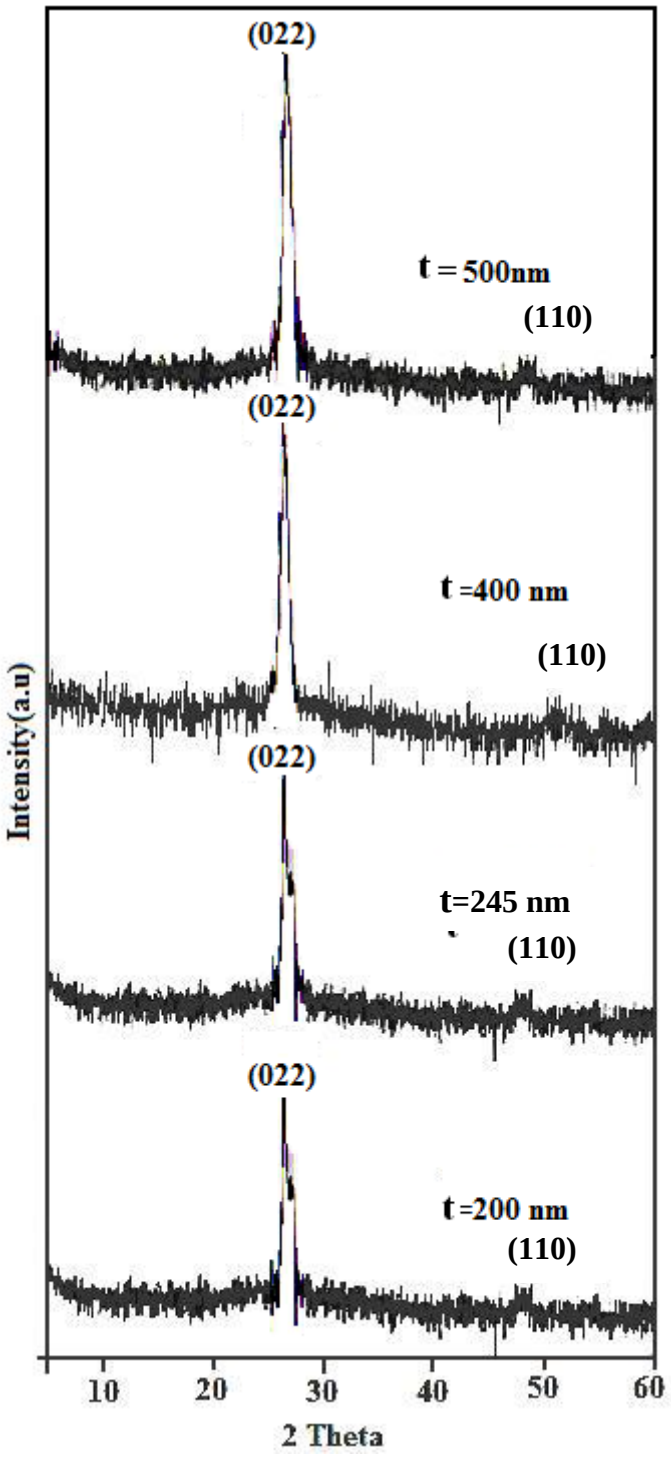

Fig.1. XRD patterns of CdS thin films of different thickness t.

Table 1. Comparison of structural parameters, FWHM, interplanar spacings, Grain size, Strain and peak intensity of the CdS thin films of different thickness t

Thickness (nm) (t±1%)	Angle 2θ	$\beta_{2\theta}$ (radian)	Interplanar spacing(d) Å	Grain size		Strain ($\varepsilon \times 10^{-4}$)	Peak Intensity (a.u)
				XRD (nm)	SEM (nm)		
200	26.420	0.0031	3.3714	49	46	7.42	280
245	26.415	0.0026	3.3707	57	65	6.68	288
400	26.423	0.0024	3.3721	62	71	6.18	305
500	26.411	0.0022	3.3728	68	72	5.69	467

In order to study the effect of film thickness, the grain size and strain in thermally evaporated CdS thin films on glass substrate versus film thickness are shown in Fig. 2. It is observed that the crystallite size increases rapidly from 200 to 250 nm and then gradually increases up to 500 nm with the increase in thickness. The intensity of the XRD peak is also found to increase with increase in film thickness. The strain decreases with the increase of film thickness, such a decrease in strain reflects the decrease in the cohesive force between film and substrate material. Therefore, we may conclude that there is a decrease in the lattice imperfections with increase in film thickness and an increase in the crystallite size [19].

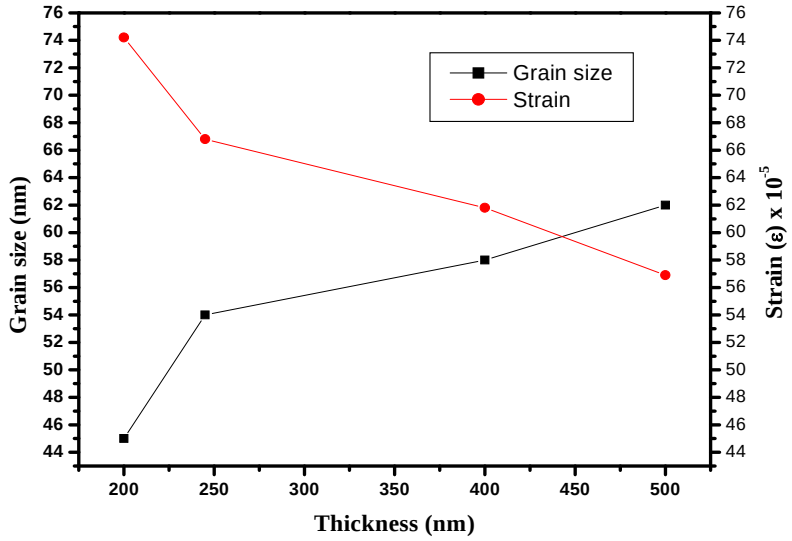

Fig. 2. Effect of thickness t on grain size and strain of CdS thin films.

3.2 SEM analysis

The microstructure of these thin films prepared by the thermal evaporation process was examined by SEM. The SEM micrographs of synthesized thin films are shown in Fig. 3. The SEM micrographs show typical tightly adherent CdS films on ultrasonically cleaned glass substrates. In most cases the final films are homogeneous, without any crack, rather dense and exhibit almost complete coverage of the substrate. They are composed of irregular shaped grains of diameter 46–72 nm. The average crystallite sizes are found to be 52 nm, confirming nanometer grain size in the cadmium sulfide films. These values are similar with the values estimated from the XRD analysis.

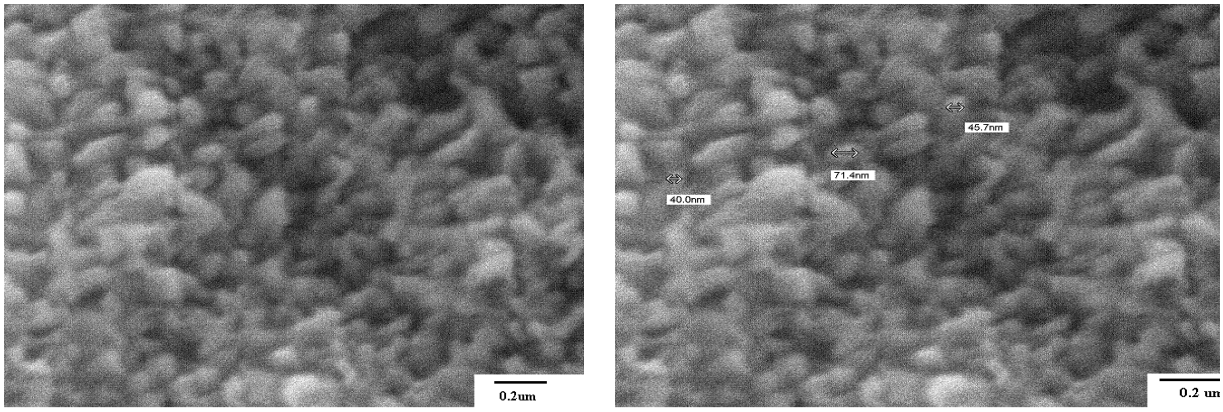

Fig. 3. SEM micrographs of thermally evaporated CdS thin films.

3.3 Optical properties of thermally evaporated CdS thin films

We have used four samples of thermally evaporated CdS thin films with the thicknesses of 200, 245, 400 and 500 nm. Optical absorbance and transmittance spectra of the films are given in Figs. 4 and 5, respectively.

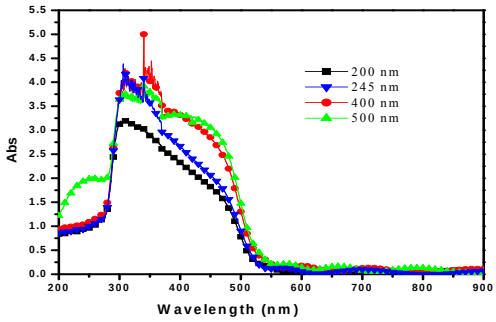

Fig. 4. Absorbance spectra of CdS thin films of different thickness t.

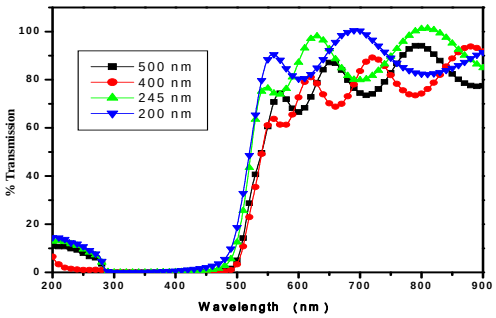

Fig. 5. Transmission spectra of CdS thin films of different thickness t.

Interference fringes are seen in these spectra. The optical band gap E_g is estimated by using the following relation [20]:

$$(\alpha h\nu)^m = A\,(h\nu - E_g) \qquad (4)$$

where A is a characteristic parameter independent of photon energy, hν is the incident photon energy and m is a constant which depends on the nature of the transition between the top of the valence band and bottom of the conduction band. The lowest optical band gap energy in semiconducting materials is referred to as the fundamental absorption edge and nature of interband transition is characterized by m [21]. For allowed indirect transition m=1/2 and for the allowed direct transition m=2. By plotting $(\alpha h\nu)^2$ versus the incident photon energy (hν) and extrapolating the straight-line portion of the plots toward low energies, the optical band gap can be obtained as shown in Fig. 6. These plots indicate that the wider linear regions are observed for the allowed direct transition (m=2) for the polycrystalline CdS thin films. The value of optical band gap energy for different film thickness is found to be in the range of 2.35-2.45 eV. The values of absorption coefficient, band gap, and Urbach's energy obtained at different thickness of the investigated samples of the films are given in table 2. On the basis of experimental results we may conclude that band gap of thin films is also thickness dependent. Here we observed that the band gap of the

thin films increases on increasing the thickness of the films. Fig. 7 shows the variation of the band gap of the film with the increase in film thickness and it increases gradually for the thickness in the 200-400 nm range and then increases abruptly for the film thickness in 400-500 nm range.

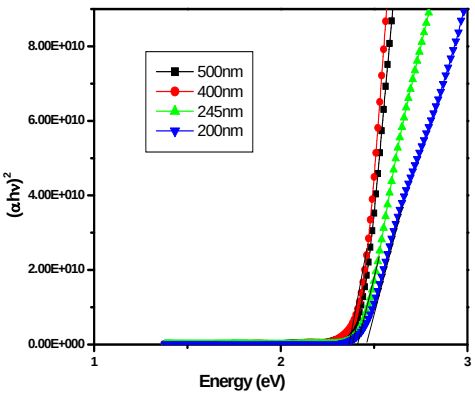

Fig. 6. The $(\alpha h\nu)^2$ versus hν graph of CdS thin films of different thickness t.

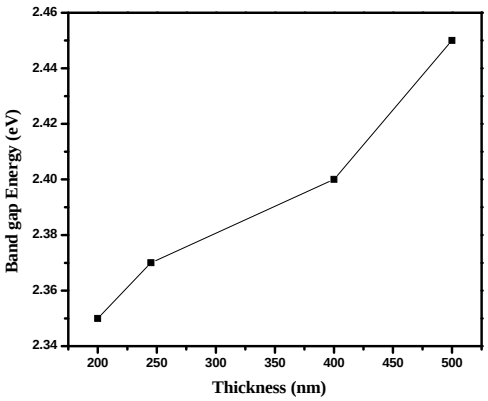

Fig.7. Effect of thickness on band gap energy.

Table 2. Absorption coefficient, Band gap, Urbach's energy of CdS thin films of different thickness t.

Thickness(nm) (t±1%)	α (cm^{-1}) at 2.5 eV	α (cm^{-1}) at 3.44 eV	Band gap (eV)	Urbach' s energy(eV)
200	8.73×10^4	19.40×10^4	2.35	0.10
245	7.96×10^4	18.37×10^4	2.37	0.12
400	5.40×10^4	16.75×10^4	2.40	0.13
500	4.47×10^4	13.51×10^4	2.45	0.190

The absorption coefficients of these films at different energies are shown in Fig. 8. A close examination of Fig. 8 reveals that the thick films have lower α value at high energy region than the thin films. The absorption coefficient shows oscillatory behaviour at the forbidden gap region. It is also observed that the thinner films have high α value in the band-to band absorption region. This effect may be explained by proposing that thicker films have bigger crystallites (grains), so they are closer to bulk crystalline CdS, but bigger grain sizes results in larger unfilled inter-granular volume so the absorption per unit thickness is reduced. The logarithm of the absorption coefficient α(ν) is plotted as a function of the photon energy (hν) for thermally evaporated CdS thin films and is shown in Fig. 9. The values of the Urbach' s energy (E_u) were calculated by taking the reciprocal of the slopes of the linear portion in the lower photon energy region of these curves and the values so obtained for various film thickness are presented in table 2. The Urbach's energy is found to increase with the increase in film thickness. This suggests that the crystalline nature of the thin films increase with the increase in film thickness and further supports increased crystalline nature as implied from the enhanced peak intensity of the XRD peaks for large film thickness.

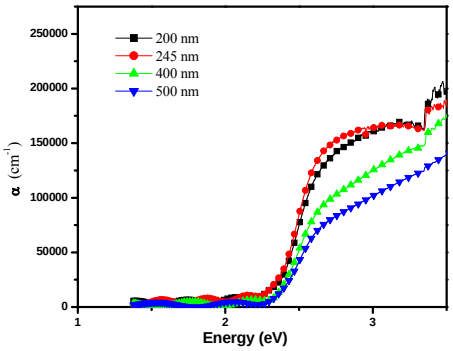

Fig. 8. The α versus hν graphs of CdS thin films of different thickness t.

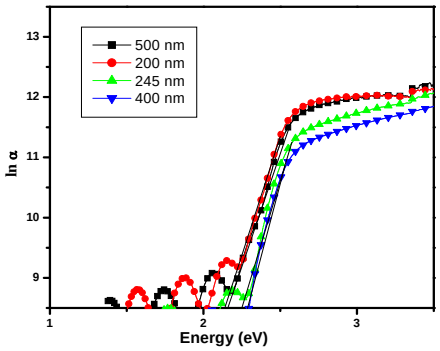

Fig. 9. The dependence of the natural logarithm of α on photon energy for CdS thin films of different thickness t.

The Extinction coefficient k of the thin films is also calculated using the formula:

$$\alpha = \frac{4\pi k}{\lambda} \tag{5}$$

where k is the extinction coefficient.

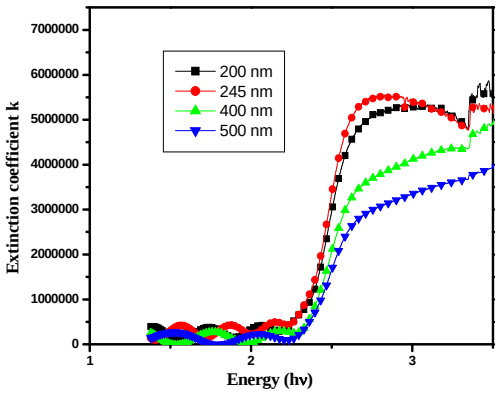

Fig. 10. Variation of k with photon energy for different film thickness t.

Variations of extinction coefficient as a function of photon energy are shown in Fig. 10. The rise and fall of the extinction coefficient in the forbidden gap region is directly related to the absorption of light. In the case of polycrystalline films, extra absorption of light occurs at the grain boundaries. This leads to non-zero value of k for photon energies smaller than the fundamental absorption edge.

4. Conclusion

CdS thin films prepared by thermal evaporation technique on glass substrate are found to be polycrystalline. Films have been characterized using optical and structural measurements. All the films exhibit high transmittance (~ 70 - 85 %), and low absorbance in the visible/ near infrared region from ~ 500 nm to 900 nm, thus making the films suitable for optoelectronic devices, for instance as window layers in solar cells. The films show a direct transition in the range 2.35 – 2.42

eV. XRD studies show hexagonal wurtzite structure of the thin films. The crystallites sizes measured by XRD studies are found to be within 49-68 nm, and those observed from SEM, are within 46-72 nm. The deductions are made to obtain the optical and structural parameters such as the optical band gap energy, absorption coefficient, extinction coefficient, Urbach's energy and grain size etc. The variations of these with thickness of thin films have been studied.

Acknowledgement

The authors are thankful to Crystal Growth Lab, Jamia Millia Islamia for extending X-ray diffraction facilities for the present work.

Reference

[1] X. Mathew, J. Pantoja Enriquez, A. Romeo, A.N. Tiwari, Sol. Energy **77,** 831 (2004).
[2] R. K. Sharma, K. Jain, A.C. Rastogi, Curr. Appl. Phys. **3**, 199 (2003).
[3] B. Ullrich, J. W. Tomm, N. M. Dushkina, Y. Tomm, H. Sakai, Y Segawa, Solid State Commun. **116**, 33 (2000).
[4] J. Brit., Ferekides, Appl. Phys. Lett. **62**, 2851 (1993).
[5] K. Tetsuya, G.Q. Guan, Y. Akira, Chem. Phys. Lett. **371**, 563 (2003).
[6] Sunny Mathew, K. P. Vijay Kumar, Bull. Mater. Sci. **17**, 235 (1994).
[7] K. Senthil, D. Mangalraj, S. K. Narayandass, Appl. Surf. Sci.**169**, 476 (2001).
[8] P. Taneja, P. Vasa, P. Ayyub, Mater. Lett. **54**, 343 (2002).
[9] S. Bhushan, S. K. Sharma, J. Phys. D: Appl. Phys. **23,** 909 (1990).
[10] M.C. Baykul, A. Balcioglu, Microelectron. Eng. **51,** 703 (2000).
[11] M. Tsuji, T. Aramoto, H. Ohyama, T. Hibino, K. Omura, J. Cryst. Growth **214,** 1142 (2000).
[12] S. Yoshihiko, O. Takashi, J. Vac. Soc. Jpn. **43**, 284 (2000).
[13] J. Nishino, S. Chatani, Y. Uotani, Y. Nosaka, J. Electroanal. Chem.**473**, 217 (1999).
[14] R.Padmavathy, N.P. Rajesh, A. Arulchakkaravarthi, R. Gopalakrishnan, P. Santhanaraghavan, P. Ramasamy, Mater. Lett. **53**, 321 (2002).
[15] I.S. Elashmawia, N. A. Hakeem, M. Soliman Selim, Mater. Chem. Phys.**115**, 132 (2009).
[16] K. Ravichandran, P. Philominathan, Appl. Surf. Sci. **255**, 5736 (2009).
[17] N. Tigau, Cryst. Res. Technol. **43,** 964 (2008).
[18] V. Bilgin, S. Kose, F. Atay, I. Akyuz, Mater. Chem. Phys. **94**, 103 (2005).
[19] E.R. Shaaban, N. Afifyb, A. El-Tahera, Journal of Alloys and Compounds **482**, 400 (2009).
[20] Titipun Thongtem, Anukorn Phuruangrat, Somchai Thongtem, Mater. Lett. **61**, 3235 (2007).
[21] J. Lee, Thin Solid Films **451-452**, 170 (2004).